# ALMA Memo ???
# Dependence of Image Quality on Antenna Number

M.A. Holdaway
NRAO/Tucson

September 26, 2004

**Abstract**

We investigate the dependence of image quality on the number of antennas in the ALMA array for single configuration case with 0.1 arcsec resolution. Five different model images are simulated with each of five different arrays with 60, 57, 54, 41, and 48 antennas. The simulated data are then imaged with two different deconvolution algorithms: Clark CLEAN (CLEAN) and Maximum Entropy (MEM). The reconstructions are evaluated with the typical methods: off-source dynamic range, on-source dynamic range, and on-source fidelity. No errors are added to the visibilities, so the results of these simulations reflect only the effects of Fourier plane coverage.

A significant decline in the quality of the deconvolved image occurs as we decrease the number of antennas in the array. However, there are two weakness to using these results to argue for 60 antennas over 50 antennas:

- even with a smaller number of antennas, the imaging quality will probably meet the imaging demands for the vast majority of observations.
- rather than being dominated by deconvolution errors due to incomplete Fourier plane coverage, ALMA images will usually be dominated by thermal noise, pointing errors, or residual phase errors.

## 1 Introduction

The number of antennas in the MMA, 40, was largely justified by (a) a desire for a given amount of collecting area (2000 $m^2$, ie, sensitivity, plus what was thought to be politically possible) combined with a cost optimization for the dish diameter, and (b) a desire for complete instantaneous $(u, v)$ coverage at an interesting resolution (about 1 arcsecond) for high quality snapshot mosaics.

The number of antennas in the ALMA array, 60 (plus 4 dedicated total power antennas), was arrived at by a desire for great sensitivity and cost optimization for the dish diameter. Apart from sensitivity, there was no explicit justification for 60 antennas (as opposed to 55 or 50) in terms of image quality. The ALMA project was funded for 64 antennas.

At this point, the antenna bids exceed our initial estimates for the antenna cost, and we may be forced to scale down the project from 60 array antennas to a lower number. The affect of such a move on sensitivity is easily calculated, but such an effect is incremental: if we reduce the number of antennas by a multiplicative factor $f$, we can reach the same sensitivity level as

the unreduced array by observing longer by a factor of $f^{-2}$. This is a slippery slope with no firm toeholds.

So, it was considered that we should also investigate the imaging properties of arrays with reduced numbers of antennas. Potentially we could get more leverage with $(u, v)$ coverage arguments, as the number of baselines goes approximately as $N_{ants}^2$. We present the results of a preliminary investigation of image quality with $N_{ants}$.

# 2 The Simulations

## 2.1 The Configurations

We seek to quantify the degradation of image quality as antennas are taken away from the ALMA. As the Conway configurations have three spiral arms, we decrease the number of antennas in the array in steps of 3, to get configurations with 60, 57, 54, 51, and 48 antennas. The ground rules we were given: perform single configuration and single pointing imaging with arrays of different numbers of antennas, but each with the same 0.1 arcsec resolution and the same shortest baseline coverage (deficiencies in the short baseline coverage can easily dominate imaging errors). Conway's configuration number 26 yields a naturally-weighted resolution of about 0.09 arcsec, which we can taper to achieve the desired 0.1 arcsec resolution. From configuration 26, we removed antennas that were not involved in the shortest spacings or the longest spacings.

As the reduced-antenna configurations have not been optimized, these simulations will not provide the best images possible, but will provide a general idea of how the image quality will degrade as the number of antennas is reduced. In Figure 1 we plot the rms sidelobe level of the PSF for a 4 hour observation as a function of the number of antennas in the array, along with a fit function which indicates the rms sidelobe level is proportional to $N_{ants}^{-1.18}$. This is sort of a sanity plot which indicates that the reduced antenna number configurations we chose represent reasonable arrays. Kogan has demonstrated that the largest negative sidelobe for a snapshot beam goes like $N_{ants}^{-1}$, so we might expect the rms sidelobe level to have a similar behavior on $N_{ants}$, and our exponent is a bit steaper, suggesting that each configuration we make by removing three more antennas is a bit away from optimal.

## 2.2 The Model Images

In the end, only two model images were used: the optical image of M51, the H $\alpha$ image of an HII region in M31. These two model sources are a nice pair for simulations work because the M51 image is dominated by pointy things, with some extended fluff around them, while the M31 image is dominated by the extended fluff, with a few embedded blobs. We needed to make images with 0.1 arcsec resolution, so we used 0.03 arcsec pixels. Each model image originally occupied a 256x256 grid, so each model image is 7.68 arcsec on a side. While these images are not huge, they are almost $\lambda/2D$ for our simulated observing frequency of 300 GHz – ie, they almost require mosaicing. In spite of our efforts to get good short spacing $(u, v)$ coverage, the 256x256 images were limited by the short spacing coverage (the shortest baseline measured between 0.54 and 0.82 of the total image flux), so we regridded the initial 256x256 images onto a 128x128 image and shrank the pixels back to 0.03 arcsec. The shortest baseline then measured

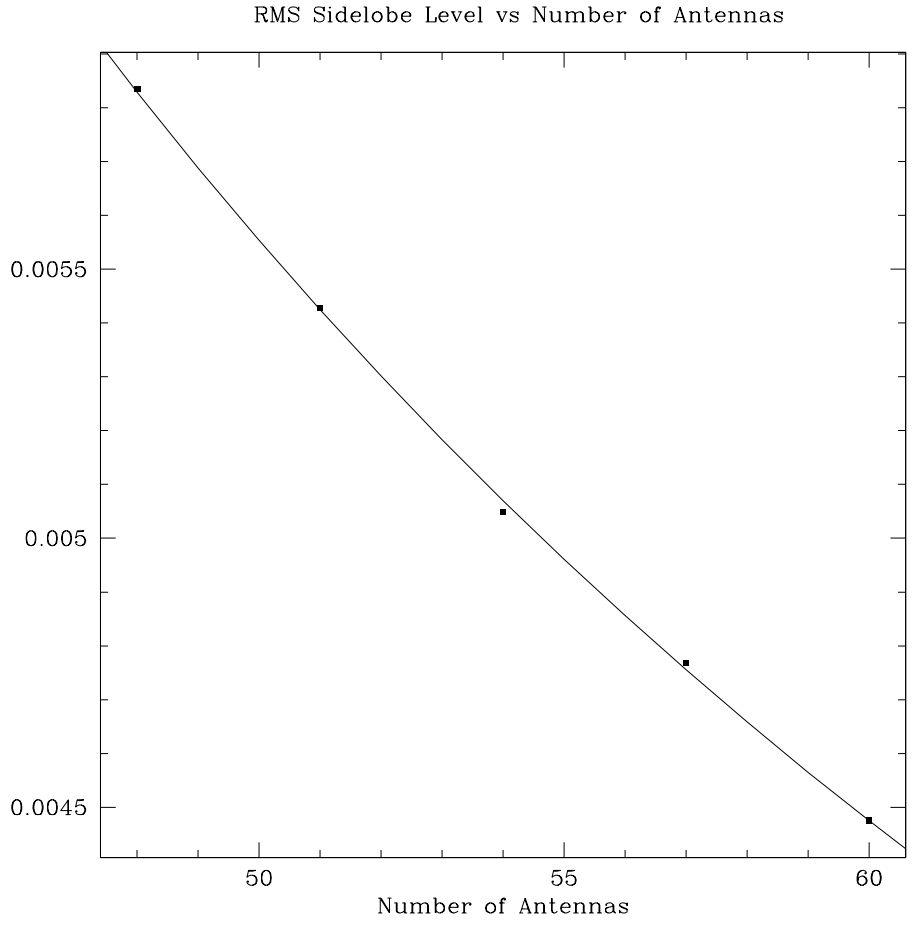


Figure 1: RMS sidelobe level of the 4 hour naturally-weighted PSF as a function of the number of antennas in the array configuration.

0.9 of the total flux or better (usually, the deconvolution can recover more flux than is present on the shortest baseline, and this is sufficient to make an excellent image reconstruction).

### 2.3 Observation Details

We simulate observations at $\delta$ = -48 deg between hour angles of -2 and +2 hours. ALMA will be a "near-transit" instrument, because the airmass, opacity, and atmospheric noise will increase greatly as you move away from transit. These 4 hour observations represent a case were we are trying to achieve excellent Fourier plane coverage and an excellent image reconstruction.

The outer (u,v) points move most quickly through the Fourier plane and require an integration time of 30 s. Every 300 seconds, we leave a 60 s gap representing calibration. No primary beam is used in the simulations. The model image is inverse Fourier transformed and degridded at the (u,v) points specified by earth rotation synthesis for each particular array. As we are primarilly interested in how the degraded (u,v) coverage could limit imaging, we do not add thermal noise or any other errors to the simulated data.

### 2.4 Processing Details

The simulated data are first gridded and Fourier transformed with natural weights plus a taper to make the dirty image and the dirty beam, each 256x256. The taper is calculated to result in a circular beam fit of precisely 0.1. A mask image (ie, a flexible CLEAN BOX) aids in the decolvolution. For ALMA, many sources which are observed at a resolution as high as 0.1 arcsec will have been observed previously at lower resolution. Hence, we assume that to within 5 resolution elements, we know where the emission will be located, and we generate a mask which is the shape of the source, extended outward by 15 pixels.

For CLEAN, the deconvolution improves the images for about 150,000 iterations, at which point the algorithm's convergence stalls (ie, the maximum residual is chaotic with iteration number).

For MEM, a noise level of 0.2 Jy was used because it was never reached in 800 iterations. No source showed divergence in the 800 MEM iterations, though there is significant chaotic behavior in the MEM fit and the MEM image quality with iteration number (this is a 10

## 3 Evaluation

We evaluate the image quality with these measures:

- **frac** is the fraction of the model flux recovered with the masked region.
- **DR1** is the off-source dynamic range, defined as the image peak divided by the off-source RMS in the image; off-source is defined by the deconvolution mask and excludes positions within five resolution elements of the true source emission.
- **DR2** is the on-source dynamic range, defined as the image peak divided by the on-source RMS error. The on-source error is defined as the true model image convolved with the 0.1 arcsec beam, minus the restored deconvolved image, and the RNS is calculated only within the imaging mask (so there is actually a band five resolution elements wide of just-off-source pixels contributing to the on-source RMS).

| CLEAN | | | | | |
|---|---|---|---|---|---|
| N | frac | DR1 | DR2 | FID01 | FID001 |
| 60 | 0.99973 | 9103 | 4635 | 625 | 380 |
| 57 | 0.99958 | 8230 | 3901 | 516 | 299 |
| 54 | 0.99952 | 6069 | 2950 | 421 | 252 |
| 51 | 0.99951 | 5208 | 2561 | 398 | 229 |
| 48 | 0.99952 | 5007 | 2621 | 397 | 232 |
| MEM | | | | | |
| N | frac | DR1 | DR2 | FID01 | FID001 |
| 60 | 1.0000 | 59887 | 54160 | 8228 | 4883 |
| 57 | 0.9999 | 46191 | 51696 | 7541 | 4276 |
| 54 | 0.9999 | 46328 | 52399 | 7042 | 4386 |
| 51 | 0.9999 | 27251 | 42173 | 6570 | 3797 |
| 48 | 0.9999 | 24999 | 38631 | 6044 | 3716 |

Table 1: Evaluation measures of the M31 model image for CLEAN and MEM deconvolution. This model image is dominated by extended emission.

- **fid01** is the fidelity of the image emission greater than 0.01 of the peak emission. Think of this as the typical SNR you have in a pixel in the reconstructed image. The image fidelity, like **DR2**, is a measure of the on-source reconstruction quality. It is the median of the fidelity image, which is the model image divided by the absolute difference between the reconstruction and the model image. Pixels in the model image with less than 0.01 of the peak model flux are not included in the median calculation.
- **fid001** is the fidelity of the image emission greater than 0.001 of the peak emission.

The evaluation measures of the M31 model simulations for CLEAN and MEM deconvolution are given in Table 1, and the evaluation measures of the M51 model simulations for CLEAN and MEM deconvolvution are shown in Table 2.

| CLEAN | | | | | |
|---|---|---|---|---|---|
| N | frac | DR1 | DR2 | FID01 | FID001 |
| 60 | 0.99984 | 20470 | 10982 | 705 | 421 |
| 57 | 0.99978 | 21644 | 11492 | 755 | 433 |
| 54 | 0.99992 | 20910 | 11370 | 749 | 435 |
| 51 | 0.99974 | 19777 | 10526 | 667 | 406 |
| 48 | 0.99969 | 19357 | 10420 | 680 | 394 |
| MEM | | | | | |
| N | frac | DR1 | DR2 | FID01 | FID001 |
| 60 | 1.00013 | 24839 | 15514 | 1145 | 662 |
| 57 | 0.99991 | 23997 | 16332 | 1183 | 655 |
| 54 | 0.99977 | 22064 | 15264 | 1060 | 605 |
| 51 | 0.99955 | 22992 | 16033 | 1067 | 617 |
| 48 | 0.99938 | 19973 | 14150 | 949 | 530 |

Table 2: Evaluation measures of the M51 model image for CLEAN and MEM deconvolution. This model image has much more compact structure than the M31 model.

In Figures 2-5 we show plots of the dynamic range DR1 and the fidelity FID01 are shown for the M31 and M51 models, with each plot showing both MEM results (in dashes and open boxes) and CLEAN results (in solid lines and solid boxes). (Note that the raw imaging power of MEM greatly outperforms CLEAN – MEM is just better at imaging extended structure than CLEAN. You may ask why MEM is not more widely used in radio astronomy. The answer lies in the positivity bias in MEM. When the SNR dips, as in most realistic observations, MEM's positivity bias prohibits negative noise but permits positive noise, effectiving converting noise into signal and resulting in an overestimate of the flux, making quantitative analysis difficult. However, do not dismiss our current MEM results on the basis of the positivity bias: any source which is bright enough to permit dynamic range of 20000:1 will have enough SNR to make the positivity constraint irrelevant.) In all these cases, there is a significant trend towards better image quality as we go to larger number of antennas. However, is this result of significance to the ALMA project?

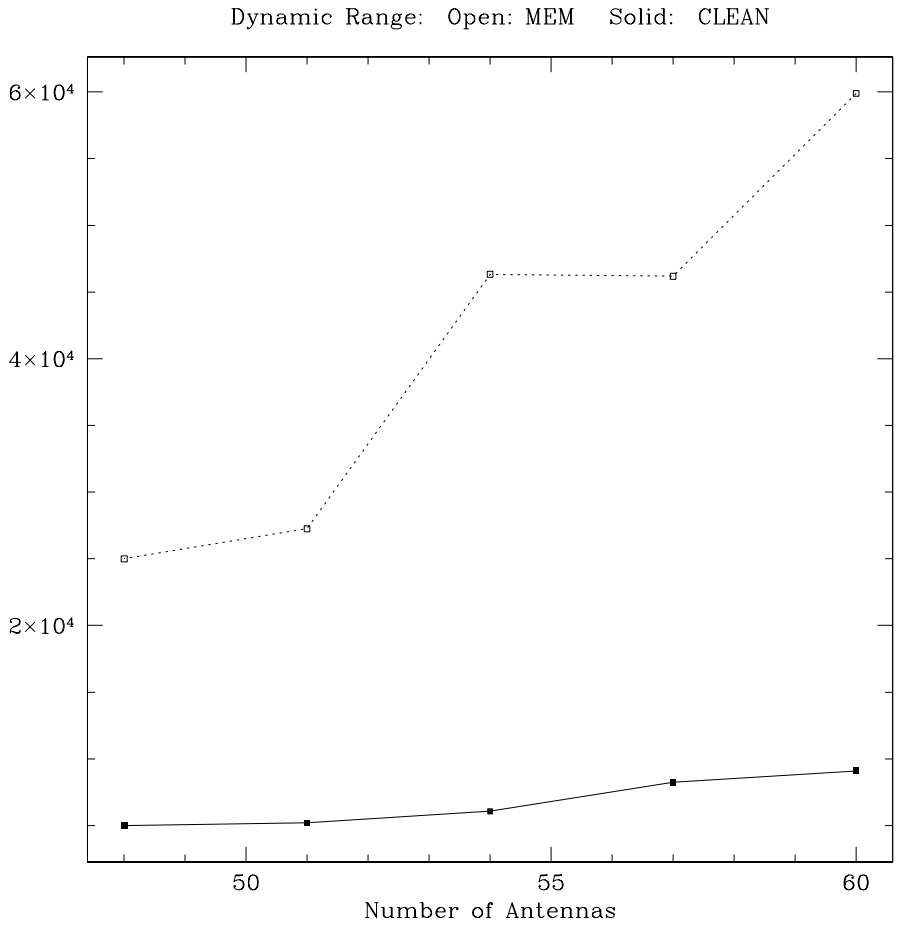


Figure 2: The DR1 dynamic range as a function of number of antennas for the M31 model simulations.

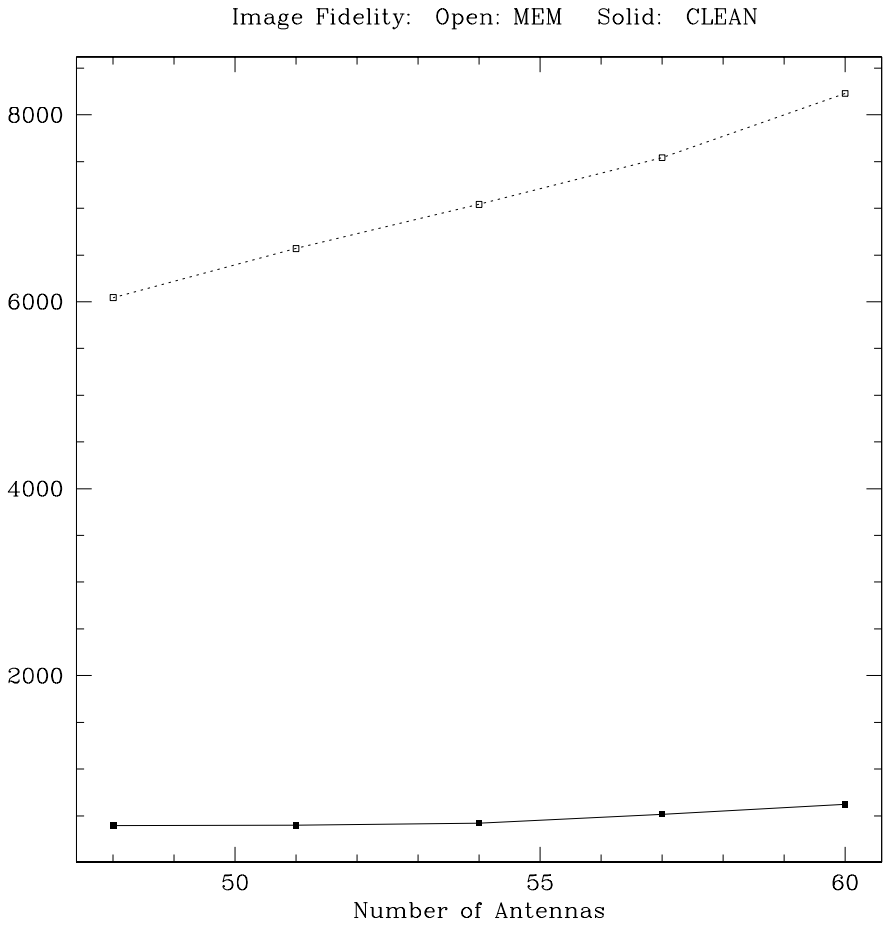


Figure 3: The FID01 dynamic range as a function of number of antennas for the M31 model simulations.

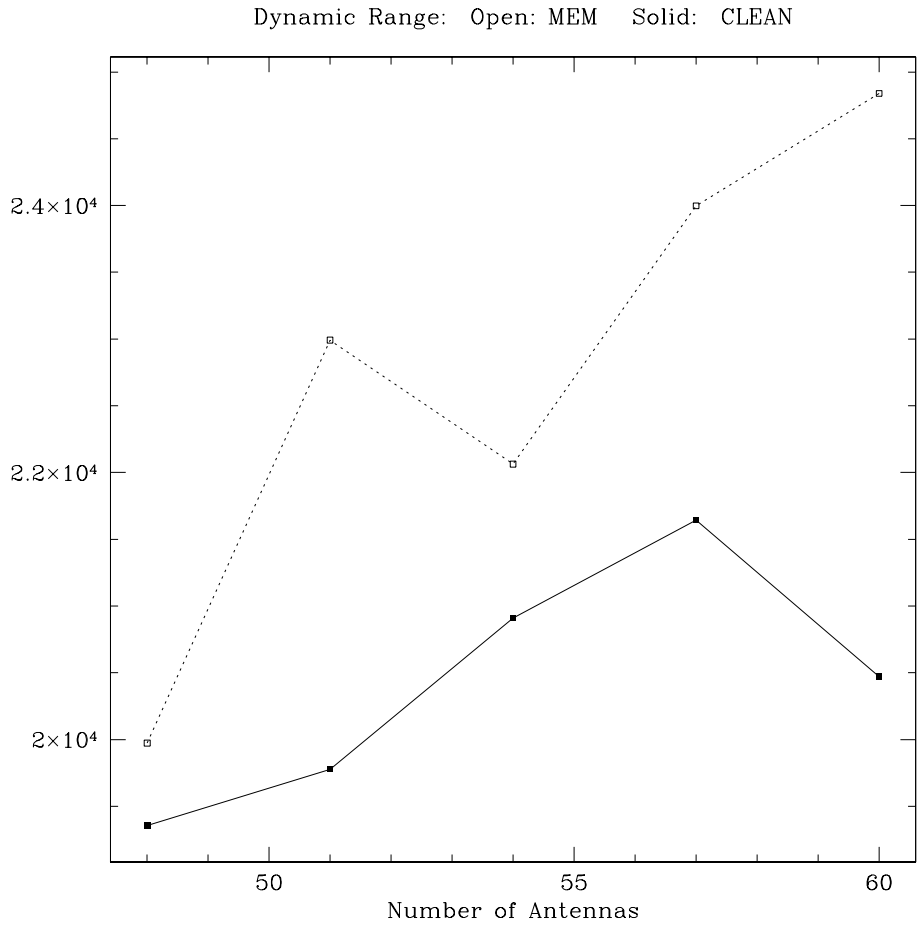


Figure 4: The DR1 dynamic range as a function of number of antennas for the M51 model simulations.

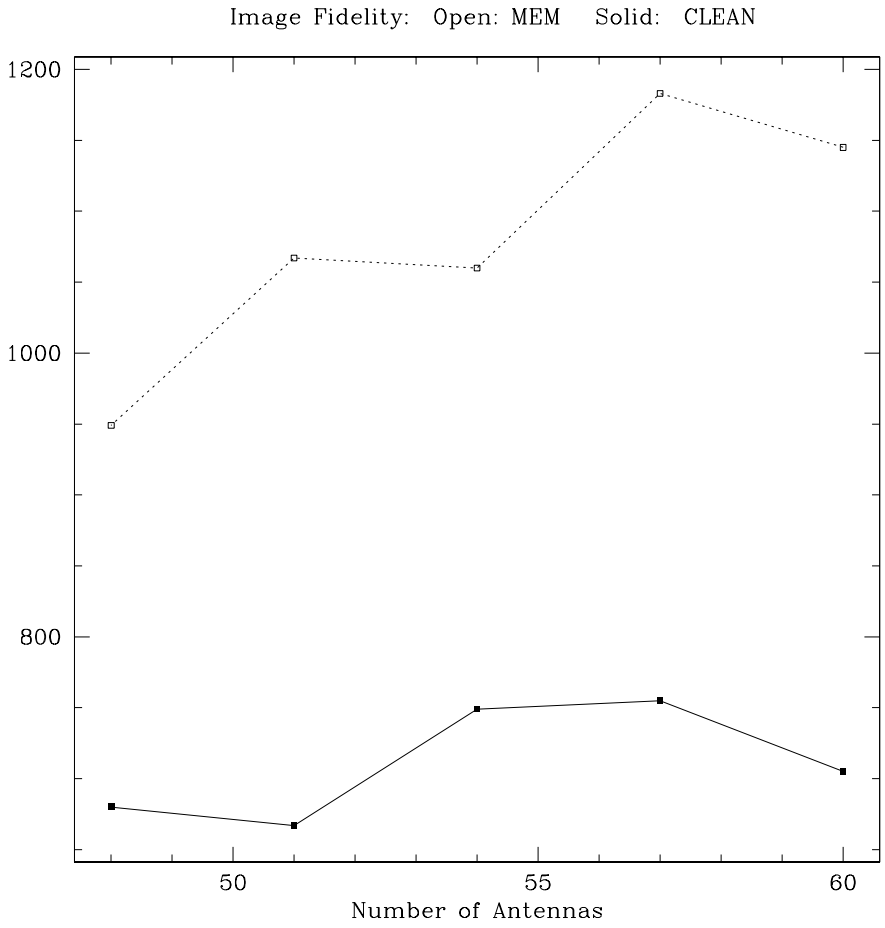


Figure 5: The FID01 dynamic range as a function of number of antennas for the M51 model simulations.

## 4 My Perspective On These Results

As most of the science ALMA plans on performing will be moderate to low SNR, we can be assured that most images produced by ALMA will not be limited by deconvolution errors, no matter the number of antennas in the array. If we take many more antennas away from ALMA, eventually we will reach a configuration which is sparse enough to significantly impact ALMA's imaging capabilities for more typical observations, but we cannot say at what point that happens. However, the modest declines in image quality seen in these simulations indicate to me at least that we do not have a requirement of 60 antennas from imaging considerations. For example, look at the DR1 of the M31 image: how often will we need to achieve a dynamic range of more than 25000 (ie, the dynamic range of the 48 antenna simulation as deconvolved by MEM)? While there will be some demanding observations which will push ALMA's array configurations, I believe gaps in the Fourier plane coverage will usually not limit the quality of ALMA's "long track" images. Rather, I expect thermal noise to limit most ALMA images, followed by the results of uncorrected pointing errors, atmospheric-opacity- induced amplitude fluctuations, residual phase errors, and for mosaics and at high frequencies, the results of uncorrected beam errors (for example, due to surface errors).